

Fractional Brownian Motion in Crowded Fluids – Supplement

Dominique Ernst¹, Marcel Hellmann², Jürgen Köhler¹, and Matthias Weiss²

¹ *Experimental Physics IV, University of Bayreuth, D-95440 Bayreuth, Germany and*

² *Experimental Physics I, University of Bayreuth, D-95440 Bayreuth, Germany*

I. EXPERIMENTAL APPROACH

Fluids for SPT experiments were obtained by dissolving dextran (500 kDa, Sigma) and sucrose (342 Da, Roth) in millipore water at concentrations of about 430 mg/ml (30% w/w) and 1500 mg/ml (60% w/w), respectively. Rhodamine-tagged tracer beads (50 nm, Polysciences) were added from a predissolved solution, resulting in a typical concentration of about 2 pM. Hence, 3-5 beads were observed in the focal plane of the microscope's widefield image ($80 \times 80 \mu\text{m}^2$).

About 35 μl of each sample was placed between acetone-cleaned coverslips and sealed on the edges with highly viscous grease to prevent evaporation or adhesion forces that would induce a flow field.

Tracking experiments were performed with a home-built single-particle tracking setup (Fig. 1) using a novel tracking technique [1–5]. Here we only describe the basic concept, technical details will be presented elsewhere.

The output of an Ar/Kr-Ion laser (Innova 70C Spectrum, Coherent) at a wavelength of 514nm with a circular polarisation (due to a $\lambda/4$ -waveplate) was used as an excitation light source. The laser beam was directed through a series of two perpendicularly arranged acousto optical deflectors (AOD, DTSX-400-532, Pegasus), responsible for the generation of an orbiting laser beam with rotation frequency f . The rotating laser beam was then passed through a telecentric lens system and directed into a home-built confocal microscope. The laser light was reflected by a dichroic beamsplitter (z532RDC, AHF) towards an infinity corrected water-immersion objective (UPLSAPO, 60x, NA=1.2, Olympus). The sample with the diffusing tracer particles was mounted on top of a three-dimensional piezo stage. This setup allowed us to create an orbit radius R in the range of 0 to $5 \mu\text{m}$ in the focal plane of the objective. Suitable dye-labeled particles in the vicinity of the rotating focal spot were excited. The emitted light was collected by the same objective, passed the dichroic beamsplitter and a further dielectric filter (HQ525LP, OD=6 @ 514nm, AHF) to suppress remaining laser light. Finally it was focussed either onto the chip of a CCD (sencam qe, PCO) or an avalanche photodiode (APD, SPCM-AQR-14, Perkin Elmer) with a sensitive area of $180 \mu\text{m}$ in diameter.

The setup was capable of working in a widefield and a confocal operation mode. For the widefield mode an optional lens in front of the microscope was flipped into the optical path to defocus the excitation to an area of about $80 \times 80 \mu\text{m}^2$ in the plane of the sample. In this mode the deflection unit is set to a neutral state (no deflection). The diffusing particles are located within the

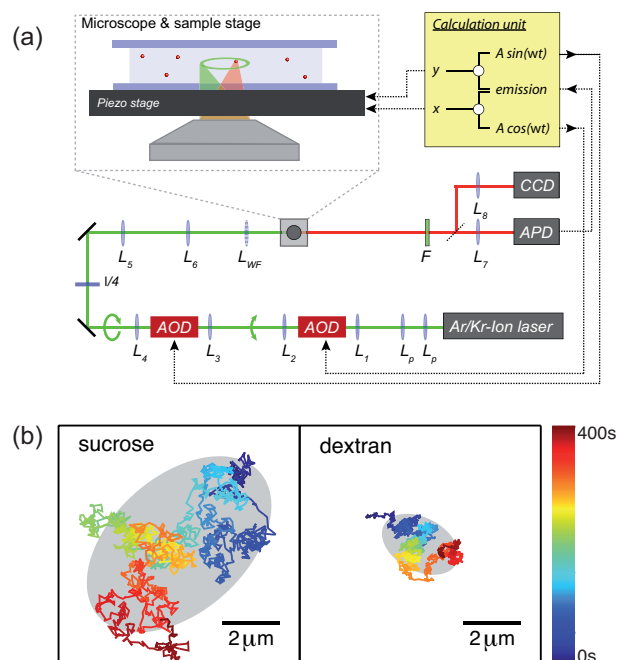


FIG. 1: (a) Sketch of the experimental setup with lenses for beam profile optimization (L_p), a widefield lens (L_{WF}), a dielectric filter (F), and an acousto optical deflector (AOD). Signals were collected either with a CCD camera or an avalanche photodiode (APD). The calculation unit provided the drive signals for the AODs, gathered the emission intensity, calculated the positions x and y , and fed the negated position to a piezo stage. (b) Representative trajectories in a purely viscous sucrose solution (left) and a crowded dextran fluid (right); color-coding blue to red highlights the temporal direction of the trajectory. The gyration ellipsoids which reflect the random walks' asphericity are superimposed in grey. Due to a higher mobility in the sucrose solution, the ellipsoids differ in size.

CCD image and are moved by the piezo stage to a proper position near the centre of the laser orbit. The confocal mode is subsequently used to perform the measurements. By flipping the optional lens back, the emission is now detected with the APD and the deflection unit is switched on. The emission intensity of the moving particle is modulated with the known frequency of the laser orbit.

Using a tracking software based on a lock-in technique [1, 3] we were able to reconstruct the two-dimensional motion of particles from the frequency-modulated fluorescence signal: From the detected photons the position with respect to the orbit center was calculated, and the piezo stage was fed with a signal corresponding to the

negated position. The whole trajectory of the tracer can be reconstructed by monitoring the feedback signal of the piezo.

Experiments were done with an orbit frequency of $f = 1\text{ kHz}$. Every four periods of rotation the position was calculated resulting in a time resolution of $\Delta t = 4\text{ ms}$. The radius for best tracking performance depends on the beam waist w of the focal spot and was found to be $R = w/\sqrt{2}$ [6]. A typical width of $w = 270\text{ nm}$ lead to a radius of $R = 190\text{ nm}$.

II. EVALUATION WINDOW OF EXPERIMENTAL DATA

We have chosen to evaluate the scaling properties of the experimental data in the temporal range 50-500ms, e.g. when inspecting the MSD. Enlarging the window in which the anomaly α and the corresponding asphericity A were determined will alter the stated numbers. Extending the fit range to larger times will include more of the crossover towards the asymptotic normal diffusion and hence $\alpha \rightarrow 1$ and $A \rightarrow 4/7$. This underlines the transient nature of the anomaly. In better words, significant elastic restoring forces are only present in crowded fluids for large frequencies, i.e. for rapid motion on short length and time scales.

Extending the fit range to smaller times will include particular features of the measurement process. The accuracy of the position measurement in SPT depends on the number of photons acquired. If too few photons are detected, small diffusion steps are masked by noise and the MSD appears to converge to a constant for $t \rightarrow 0$ [7, 8]. This behavior may mimic a subdiffusive characteristics at small times ('false positives'). In our experiments photon statistics was sufficiently high to make this effect negligible, i.e. the scaling exponent of a purely viscous fluid deviated from unity only by less than 2%. But even when having enough photon statistics and normal diffusion, an apparently anomalous characteristics may emerge: Since diffusion does not stop during the acquisition process (given by the acquisition time Δt), the MSD will take on a form $\langle r(t)^2 \rangle = 4D(t - \Delta t/3)$ [9]. Due to the subtraction of a constant, the MSD hence may mimic a superdiffusive scaling for short times. To avoid all these contributions, we have restricted ourselves to the indicated fit window which is least affected by the above mentioned processes.

From the two-dimensional trajectory with N position and a time resolution of Δt , we obtained the gyration tensor via

$$T_{ij} = \frac{1}{N} \sum_{n=1}^N (r_i(n\Delta t) - \langle r_i \rangle) (r_j(n\Delta t) - \langle r_j \rangle). \quad (1)$$

Here, $\langle r_i \rangle$ denotes the i -th component of the center of mass. Diagonalizing T_{ij} yields the principal axes of gyration and the corresponding eigenvalues, i.e. the squared principal radii of gyration, R_i^2 .

III. SIMULATIONS

We have considered two different models for anomalous diffusion, namely diffusion in a percolation system (obstructed diffusion, OD) and fractional Brownian motion (FBM). Computer simulations of the respective process provide numerical values for the shape parameters that can be compared to experimental data.

Obstructed diffusion was simulated on a square lattice (350×350 sites) with periodic boundary conditions. A fixed fraction f of randomly chosen sites were occupied by static obstacles and tracer particles were allowed to move on the remaining free sites according to the blind ant algorithm (see, e.g. [10]). Depending on the occupied volume fraction f , the support becomes a fractal [11], and diffusion can become (transiently) anomalous. For a critical concentration of obstacles $f_p = 0.40726$ [12], the *percolation threshold* in two dimensions, subdiffusion with $\alpha \approx 0.69$ is observed on all time scales whereas for $f < f_p$ a transient, yet long-lasting subdiffusion with a finite-size corrected anomaly α emerges. Indeed, for $f < f_p$ normal diffusion is asymptotically restored. For $f > f_p$, tracers are confined to finite domains, i.e. an initial subdiffusion is observed but asymptotically the particle is bound to a certain region in space. In our simulations, we varied the occupied volume fraction in the range $0.33 \leq f \leq 0.42$ which resulted in straight power laws of the particles' MSD within the simulation period. For every value of f , we simulated 1.5×10^6 random walks, where for every 1000th run a new environment was created. Each random walk was started at a randomly chosen vacant site. Occasionally, particles were trapped in a small subvolume of the lattice due to the random placement of obstacles. We identified such situations and removed trapped trajectories from the analysis.

For the simulation of FBM we used the circulant method [13] which is in principle exact, i.e. the deviations between 'true' and simulated FBM are due to computational limitations like finite numerical accuracy. The method relies on the embedding of the covariance matrix of FBM into a circulant matrix that is diagonalized by a discrete Fourier transform. Using a fast Fourier transform (FFT), the simulation time for a trajectory of length N scales as $N \log N$. We generated 10^6 independent trajectories, each having $N = 2^{13}$ positions. The anomaly was varied in the range $0.5 \leq \alpha \leq 0.9$. For normal diffusion ($\alpha = 1$), we relied on Brownian Dynamics simulations [14] that are based on the overdamped Langevin equation, $\mathbf{r}(t + \Delta t) = \mathbf{r}(t) + \xi(\Delta t)$ with ξ being a random variable with white noise characteristics.

IV. RESULTS ON A TRUNCATED CTRW MODEL

To overcome the somewhat artificial features of the CTRW model due to its asymptotic scaling of the distribution of waiting times, $p(\tau) \sim 1/\tau^{1+\alpha}$, we have con-

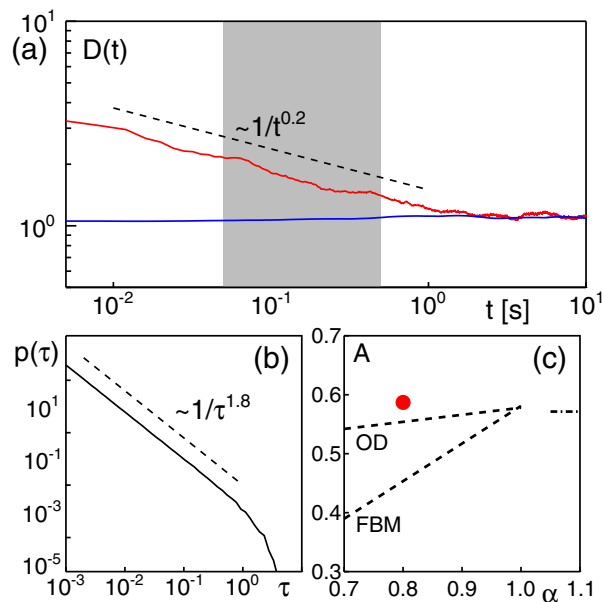


FIG. 2: (a) Representative time-averaged MSD of truncated CTRW model ($\alpha = 0.8$), shown as $D(t) = \langle r(t)^2 \rangle / t$ to highlight the asymptotic scaling. Data for the time- and ensemble-averaged MSD are shown in blue and red, respectively. For the ensemble-averaged quantity a transient scaling $D(t) \sim 1/t^{0.2}$ in the experimentally relevant interval is observed before asymptotically reaching the normal diffusion limit ($D \rightarrow \text{const.}$). Hence, the truncated CTRW model only shows transiently a weak ergodicity breaking. (b) The probability distribution function of waiting times, $p(\tau)$ used for the truncated CTRW model. After a transient power-law scaling, the distribution displays an exponential tail that enforces an asymptotic convergence of the MSD to normal diffusion. (c) The asphericity of the truncated CTRW model for $\alpha = 0.8$ (red dot) deviates considerably from the predictions of the OD and FBM models (dashed lines). It is most consistent with the limiting value $A = 4/7$ for normal diffusion and hence incompatible with the experimental data found for a crowded dextran solution.

structured a truncated CTRW model. In particular, we followed previous reports that had implied exponentially truncated power-law distributions [15]. A truncated $p(\tau)$ is expected to yield a long-lasting transient subdiffusion which asymptotically converges to normal diffusion.

We therefore have simulated a two-dimensional CTRW with $\alpha = 0.8$ and a truncated distribution of waiting times with parameters that yielded a close match with the experimental MSD data. The chosen waiting time distribution and the resulting behavior of the MSD (again shown as $D(t) = \langle r(t)^2 \rangle / t$) are reported in Fig. 2. As can be seen in Fig. 2a, the time-averaged $D(t)$ is approximately constant whereas the ensemble-averaged quantity shows a transient scaling $\sim 1/t^{0.2}$ (i.e. $\langle r(t)^2 \rangle_E \sim t^{0.8}$) before converging to the asymptotic limit of normal diffusion. Hence, the CTRW's feature of a linear scaling of the time-averaged MSD persists even for the truncated model. The associated waiting time distribution (Fig. 2b) shows a power-law decay over several orders of magnitude before being exponentially truncated.

We next determined the asphericity for the truncated CTRW model. Since the trajectory of a CTRW at any instance of time geometrically looks like the path of normal Brownian motion, we expected a value $A \approx 4/7$ for the truncated CTRW model. Indeed, our expectation turned out to be correct (Fig. 2c). Furthermore, A did not change significantly with the imposed anomaly α (data not shown). Shifting the truncation to larger and larger times resulted in a slight increase of A rather than reducing the value. Therefore, based on the scaling of $\langle r(t)^2 \rangle_T$ and the asphericity, we can not only rule out OD and the full CTRW model but also a (truncated) CTRW model as an explanation of the experimentally observed anomalous diffusion.

-
- [1] J. Enderlein, Appl. Phys. B **71**, 773 (2000).
 - [2] J. Enderlein, Single Mol. **1**, 225 (2000).
 - [3] K. Kis-Petikova and E. Gratton, Microsc. Res. Tech. **63**, 34 (2004).
 - [4] K. McHale, A. J. Berglund, and H. Mabuchi, Nano Lett. **7**, 3535 (2007).
 - [5] A. Berglund and H. Mabuchi, Appl. Phys. B **78**, 653 (2004).
 - [6] A. Berglund and H. Mabuchi, Appl. Phys. B **83**, 127 (2006).
 - [7] D. Martin, M. Forstner, and J. Kas, Biophys. J. **83**, 2109 (2002).
 - [8] M. Hellmann, D. Heermann, and M. Weiss, EPL **94**, 18002 (2011).
 - [9] M. Goulian and S. Simon, Biophys. J. **79**, 2188 (2000).
 - [10] M. Saxton, Biophys. J. **66**, 394 (1994).
 - [11] S. Havlin and D. Ben-Avraham, Adv. Phys. **36**, 695 (1987).
 - [12] M. Newman and R. Ziff, Phys. Rev. Lett. **85**, 4104+ (2000).
 - [13] A. Wood and G. Chan, J. Comp. Graph. Stat. **3**, 409 (1994).
 - [14] D. Ermak, J. Chem. Phys. **62**, 4189 (1975).
 - [15] C. Gonzalez, MC and Hidalgo and A. Barabasi, Nature **453**, 779 (2008).